Barankin Bound vs Cramér-Rao Bound for Interferometric-Like Array Design at Low SNR

Jianhua Wang*, Lucien Bacharach*, Mohammed Nabil El Korso†, Pascal Larzabal*

* SATIE, Université Paris-Saclay, 91190 Gif-sur-Yvette, France
† L2S, Université Paris-Saclay, 91190 Gif-sur-Yvette, France

Abstract—In this paper, we address the antenna array design problem at low signal-to-noise ratio (SNR). The Cramér-Rao bound (CRB) is the most commonly used criterion to solve the array optimization problem due to its computing simplicity and tightness in the asymptotical region. However, there exists a threshold SNR at which the estimation variance significantly deviates from the CRB. In this case, the CRB is no longer a tight bound. To address this issue, we propose the use of the Barankin Bound (BB) on the source location and source intensity in astrometry and photometry problems as an alternative optimization criterion. BB provides a mean square error (MSE)-optimal trade-off mainlobe width and sidelobe level of beampattern. The performance of the obtained array geometries is assessed and compared by evaluating the aforementioned bounds and the mean square error (MSE) on the estimation of source location and intensity. The simulation results illustrate that the BB-based criterion provides a trade-off between increasing the estimation accuracy and reducing the ambiguity.

Index Terms—Barankin bound, Cramér-Rao bound, array selection, threshold SNR, performance analysis

I. INTRODUCTION

In recent decades, radio telescope arrays have grown in size, with many more antenna elements and unprecedented spatial spread. The increased number of antennas improves the resolution and sensitivity of the interferometer, such as those used in NenuFAR [1] and SKA [2]. Since the estimation accuracy of the antenna array depends essentially on the positions of the antennas, the array geometry design is a fundamental problem before putting the instrument into operation. The antenna array design problem can be solved by formulating it as an optimal selection problem over a grid [3] in order to make the solution tractable.

To solve the array selection problem, we need to evaluate the accuracy of the system in terms of MSE. However, assessing MSE requires large numbers of Monte-Carlo simulations, which can quickly become computationally expensive as the dimension of the problem increases. To overcome this difficulty, lower bounds of MSE are chosen and used as an antenna selection criterion [4]. In array processing, the Cramér-Rao bound (CRB) is commonly used as a design criterion to solve the problem of optimal antenna placement [5]–[7], due to its simplicity and existence of closed form.

However, it should be noted that CRB is only accurate at high SNR. Due to the presence of high sidelobes or grating lobes, the CRB is inaccurate at low SNR [8]. This can be a

major concern in the field of radio astronomy [9]–[11], where sources generally have low SNR. The low-SNR region is delimited by the so-called threshold or breakdown SNR, below which the performance of estimators degrades dramatically.

As one of the most powerful lower bound on the variance of an unbiased parameter estimate, the Barankin Bound (BB) can be used to predict the threshold SNR [12], below which the BB is much tighter than CRB. Theoretically, the BB is the solution of an integral equation, and thus, it generally cannot be derived in closed form. However, many approximations of the true BB have been proposed, such as the McAulay-Seidman [13], the Hammersley-Chapman-Robbins [14], and the McAulay-Hofstetter [15] bounds.

To the best of our knowledge, there is no published work in the literature regarding the use of the BB for solving the antenna selection problem at low SNR, except [16] in a Bayesian context (which is beyond the scope of our work) of cognitive antenna selection, in which the authors used a specific BB bound, namely the Bobrovsky-Zakai bound. In this paper, we will solve the antenna selection problem at low SNR by using CRB-based and BB-based design criteria. The performances of the two optimized arrays are evaluated and then compared from the perspectives of sidelobe level and MSE threshold SNR. At last, it is demonstrated that the BB-based criterion leads to better estimation performance than CRB-based criterion, especially at low SNR.

The rest of this paper is organized as follows. Section II presents the system model. In Section III, the background and derivation of the CRB and the BB are given. The problem formulation and optimization methodology are described in Section IV. Simulation setting and result analyses are presented in Section V. Finally, conclusions are drawn and future research directions are proposed in Section VI.

II. SYSTEM MODEL

An antenna array with p identical sensors is considered, in which the position of the i-th antenna is denoted by $\mathbf{r}_i = [x_i, y_i, z_i]^T$. A single, narrowband far-field source $s(t)$ centered at frequency $\omega_c = \frac{2\pi}{\lambda}$ impinges on the array. The position of the source is represented by the unit vector $\boldsymbol{\ell} = [l, m, n]^T$, where l, m and n are direction cosines. Details about the coordinate systems, which are usually used in radio astronomy as source coordinates, can be found in [17]. Consequently, the array signal vector $\mathbf{x}(t) \in \mathbb{C}^p$ reads as

$$\mathbf{x}(t) = \mathbf{a}(\boldsymbol{\ell})s(t) + \mathbf{n}(t), \qquad (1)$$

where $\mathbf{n}(t)$ is the $p \times 1$ noise vector, $s(t)$ is the scalar source signal, and $\mathbf{a}(\boldsymbol{\ell})$ is the spatial signature vector with expression

$$\mathbf{a}(\boldsymbol{\ell}) = \left[e^{-\mathrm{j}\frac{2\pi}{\lambda}d_1(\boldsymbol{\ell})}, e^{-\mathrm{j}\frac{2\pi}{\lambda}d_2(\boldsymbol{\ell})}, \ldots, e^{-\mathrm{j}\frac{2\pi}{\lambda}d_p(\boldsymbol{\ell})} \right]^T, \quad (2)$$

in which $d_i(\boldsymbol{\ell}) = \boldsymbol{\ell}^T \mathbf{r}_i$ is the propagation delay associated with the i-th antenna.

All the antenna positions can be stacked into a matrix $\boldsymbol{\Xi} = [\mathbf{r}_1, \mathbf{r}_2, \ldots, \mathbf{r}_p]^T \in \mathbb{R}^{p \times 3}$. The spatial signature vector can then be rewritten as

$$\mathbf{a}(\boldsymbol{\ell}) = \exp\left(-\mathrm{j}\frac{2\pi}{\lambda} \boldsymbol{\Xi}\boldsymbol{\ell} \right), \quad (3)$$

where the exponential function is applied element-wise to the arguments.

The random source signal $s(t)$ follows a complex Gaussian distribution with zero mean and variance σ_s^2. The noise of the antenna is assumed to be white complex Gaussian, circularly symmetric and independent of the source signal, and the noise variance σ_n^2 is here assumed to be the same for each antenna. Thus, the model of the covariance matrix is

$$\mathbf{R} = \sigma_s^2 \mathbf{a}(\boldsymbol{\ell})\mathbf{a}(\boldsymbol{\ell})^H + \sigma_n^2 \mathbf{I}_p. \quad (4)$$

In our problem, both the position and the intensity of the source need to be estimated. As a result, the unknown parameter vector reads as

$$\boldsymbol{\eta} = [l, m, \sigma_s^2, \sigma_n^2]^T. \quad (5)$$

In the following, $\boldsymbol{\eta}_0 = [l_0, m_0, \sigma_{s0}^2, \sigma_{n0}^2]^T$ represents the true value of the unknown parameter vector $\boldsymbol{\eta}$. The joint probability density function for the realization $\mathbf{x} = \{\mathbf{x}(t_1), \mathbf{x}(t_2), \ldots, \mathbf{x}(t_N)\}$ is expressed as

$$p(\mathbf{x}|\boldsymbol{\eta}) = \prod_{i=1}^{N} \frac{1}{\pi^p |\mathbf{R}|} e^{-\mathbf{x}(t_i)^H \mathbf{R}^{-1} \mathbf{x}(t_i)}, \quad (6)$$

in which $|\cdot|$ denotes the determinant operator.

For the convenience of presentation but with no loss of generality, we will focus on the planar array with $z_i = 0$ in the remainder of this paper.

III. BACKGROUND AND EXPRESSION ON MSE LOWER BOUND

Denoting an unbiased estimate of the unknown parameter vector by $\hat{\boldsymbol{\eta}}$, it is shown in [15] that

$$\mathrm{cov}(\hat{\boldsymbol{\eta}}) \geq \mathbf{C}_{\mathrm{BB}} \geq \mathbf{C}_{\mathrm{CRB}}, \quad (7)$$

where $\mathrm{cov}(\hat{\boldsymbol{\eta}}) = \mathcal{E}\{(\hat{\boldsymbol{\eta}} - \boldsymbol{\eta})(\hat{\boldsymbol{\eta}} - \boldsymbol{\eta})^T\}$ denotes the estimation error covariance matrix, $\mathbf{C}_{\mathrm{BB}}$ represents the BB matrix, $\mathbf{C}_{\mathrm{CRB}}$ is the CRB matrix, and the matrix inequality means that the difference between two matrices is a non-negative-definite matrix. In fact, in addition to the unbiasedness of the estimator at the true value, the CRB adds the constraint of first-order derivative unbiasedness in the vicinity of the true value, while the BB imposes that the estimator should be unbiased for all possible values of the unknown parameters [18]. This is why the CRB is called a local bound (i.e., at the neighborhood

of true value), while the BB is known as a global bound. Consequently, it implies that the BB is a tighter bound than CRB.

A. Cramér-Rao Bound

As mentioned above, the CRB is widely employed as an optimization criterion in the array selection problem. Minimizing the CRB contributes to decrease the mainlobe width in the beampattern, resulting in a better resolution of the estimator. However, the CRB does not take the sidelobes into account. The sidelobes increase along with the decrease of the mainlobe width, which will substantially degrade the performance of the estimator at low SNR. In this part, the formula of the CRB for our problem is given in detail.

The CRB is the inverse of Fisher information matrix (FIM), i.e., $\mathbf{C}_{\mathrm{CRB}} = \mathbf{F}^{-1}$, in which the FIM reads as [19]

$$\mathbf{F} = N \left[\frac{\partial \mathrm{vec}(\mathbf{R})}{\partial \boldsymbol{\eta}} \right]^H (\mathbf{R}^T \otimes \mathbf{R})^{-1} \frac{\partial \mathrm{vec}(\mathbf{R})}{\partial \boldsymbol{\eta}}, \quad (8)$$

in which

$$\mathrm{vec}(\mathbf{R}) = (\mathbf{a}^* \odot \mathbf{a}) \sigma_s^2 + \sigma_n^2 \mathrm{vec}(\mathbf{I}), \quad (9)$$

where $\otimes$ is the Kronecker product, $\mathrm{vec}(\cdot)$ represents the operator converting a matrix to a vector by stacking the columns of the matrix, $\odot$ is the Khatri-Rao or column-wise Kronecker product and * denotes the complex conjugation.

Then, the derivative can be written as

$$\frac{\partial \mathrm{vec}(\mathbf{R})}{\partial \boldsymbol{\eta}} = [\mathbf{J}_l, \mathbf{J}_m, \mathbf{J}_{\sigma_s}, \mathbf{J}_{\sigma_n}], \quad (10)$$

where

$$\begin{aligned} \mathbf{J}_l &= \mathrm{j}\frac{2\pi}{\lambda} \left(\mathbf{D}_x \mathbf{a}^* \odot \mathbf{a} - \mathbf{a}^* \odot \mathbf{D}_x \mathbf{a} \right) \sigma_s^2 \\ \mathbf{J}_m &= \mathrm{j}\frac{2\pi}{\lambda} \left(\mathbf{D}_y \mathbf{a}^* \odot \mathbf{a} - \mathbf{a}^* \odot \mathbf{D}_y \mathbf{a} \right) \sigma_s^2 \\ \mathbf{J}_{\sigma_s} &= \mathbf{a}^* \odot \mathbf{a} \\ \mathbf{J}_{\sigma_n} &= \mathrm{vec}(\mathbf{I}), \end{aligned} \quad (11)$$

with

$$\mathbf{D}_x = \mathrm{diag}([x_1, x_2, \ldots, x_p]), \ \mathbf{D}_y = \mathrm{diag}([y_1, y_2, \ldots, y_p]).$$

B. Barankin Bound

The theoretical constraint (unbiasedness for all possible values of $\boldsymbol{\eta}$) of the original BB is neither applicable nor computable in practice [20]. As an alternative, the approximation of BB is calculated by appropriately choosing some points in the unknown parameter space, namely test points. In fact, the approximated BB is obtained by expressing the unbiasedness constraint at the test points. The approximation of BB applied in this paper is the Hammersley-Chapman-Robbins bound (HCRB) [14], with the formulas as follows

$$\mathbf{C}_{\mathrm{HCRB}} = \boldsymbol{\Phi}(\mathbf{B} - \mathbf{1}\mathbf{1}^T)^{-1}\boldsymbol{\Phi}^T, \quad (12)$$

where $\boldsymbol{\Phi} = [\boldsymbol{\eta}_1 - \boldsymbol{\eta}_0, \ldots, \boldsymbol{\eta}_L - \boldsymbol{\eta}_0]$ is the test point matrix with $\boldsymbol{\eta}_i$ denoting i-th so-called test point ($i = 1, 2, \ldots, L$, at

which the estimator is assumed to be unbiased), and $\mathbf{B}$ is the Barankin matrix with the (i, j)-th component defined by

$$[\mathbf{B}]_{i,j} = \mathcal{E}_{\mathbf{x}|\boldsymbol{\eta}_0}\{\nu(\mathbf{x}|\boldsymbol{\eta}_i)\nu(\mathbf{x}|\boldsymbol{\eta}_j)\}, \qquad (13)$$

in which

$$\nu(\mathbf{x}|\boldsymbol{\eta}_j) \triangleq \frac{p(\mathbf{x}|\boldsymbol{\eta}_j)}{p(\mathbf{x}|\boldsymbol{\eta}_0)}. \qquad (14)$$

Substituting (6) into (14) for evaluating (13) and after a few lines of algebra, it yields

$$[\mathbf{B}]_{i,j} = \left(\frac{|\mathbf{R}(\boldsymbol{\eta}_0)|^2}{|\mathbf{R}(\boldsymbol{\eta}_j)||\mathbf{R}(\boldsymbol{\eta}_i)|} \right)^N$$
$$\cdot \prod_{k=1}^N \mathcal{E}_{\mathbf{x}|\boldsymbol{\eta}_0}\left\{ e^{-\mathbf{x}(t_k)^H\left[\mathbf{R}(\boldsymbol{\eta}_j)^{-1}+\mathbf{R}(\boldsymbol{\eta}_i)^{-1}-2\mathbf{R}(\boldsymbol{\eta})^{-1}\right]\mathbf{x}(t_k)} \right\}$$
$$= \left(\frac{|\mathbf{R}(\boldsymbol{\eta}_0)|}{|\mathbf{R}(\boldsymbol{\eta}_j)||\mathbf{R}(\boldsymbol{\eta}_i)||\mathbf{R}(\boldsymbol{\eta}_j)^{-1}+\mathbf{R}(\boldsymbol{\eta}_i)^{-1}-\mathbf{R}(\boldsymbol{\eta}_0)^{-1}|} \right)^N,$$

on the condition that $\mathbf{R}(\boldsymbol{\eta}_j)^{-1} + \mathbf{R}(\boldsymbol{\eta}_i)^{-1} - \mathbf{R}(\boldsymbol{\eta}_0)^{-1}$ is a positive-definite matrix.

IV. OPTIMIZATION METHODOLOGY

A. Problem formulation

We treat here the array design as an antenna selection problem, which means we aim at determining the placement of K antennas so that optimal estimation performance of the source location and intensity can be achieved. The antenna selection problem can be formulated as an optimization problem based on some pre-defined performance measures, namely the CRB or BB in our case. Namely, the optimization problem we aim at solving is

$$\begin{aligned} \min_{\mathbf{w}} \quad & f\left(\mathbf{C}(\mathbf{w})\right) \\ \text{s.t.} \quad & \mathbf{1}_p^T\mathbf{w} = K \\ & w_i \in \{0, 1\}, \end{aligned} \qquad (15)$$

where $\mathbf{w} = [w_1, w_2, \ldots, w_p]^T$ is the selection vector, in which w_i indicates whether the i-th antenna of the initial array of p antennas is selected (i.e., $w_i = 1$) or not (i.e., $w_i = 0$), and $f\left(\mathbf{C}(\mathbf{w})\right)$ is a cost function related to the lower bound matrix $\mathbf{C}(\mathbf{w})$ chosen as optimization criterion. The cost function is minimized to select K antennas out of p available antennas. There are different types of cost functions [21], and the typical choices are:

1) *A-optimality*: $f = \text{tr}\{\mathbf{C}(\mathbf{w})\}$,
2) *E-optimality*: $f = \lambda_{\max}\{\mathbf{C}(\mathbf{w})\}$,
3) *D-optimality*: $f = \log\det\{\mathbf{C}(\mathbf{w})\}$.

The *A-optimality* is chosen here, because it minimizes the total estimation variance of the unknown parameters. It is worth mentioning that the noise intensity is a nuisance parameter in our scenario. In addition, we will consider the estimation of source position and intensity at the same time, and therefore, the antenna selection problem can be stated as:

$$\begin{aligned} \min_{\mathbf{w}} \quad & \text{tr}\left(\boldsymbol{\Psi}_{lms}\mathbf{C}\boldsymbol{\Psi}_{lms}^T\right) \\ \text{s.t.} \quad & ||\mathbf{w}||_1 = K \\ & w_i \in \{0, 1\}, \end{aligned} \qquad (16)$$

in which $\mathbf{C}$ denotes either $\mathbf{C}_{\text{CRB}}$ (the classical bound) or $\mathbf{C}_{\text{BB}}$ (our recommended bound), and $\boldsymbol{\Psi}_{lms}$ is a selection matrix extracting the bound components corresponding to the source location (l, m), and intensity σ_s^2.

B. Optimization methodology

Concerning the optimization method, the problem (16) can generally be solved directly and efficiently by using a convex approximation method [21] or greedy algorithms [3]. However, it can be difficult to apply the above methods in the case of the BB due to the necessity of using test points. Since our aim is to demonstrate the relevance of the BB with respect to the CRB as an antenna selection criterion, we define a small-dimensional problem in order to verify the feasibility and validity of our idea. In this simplified case, we can afford to use an exhaustive search method to solve the antenna selection problem.

C. Barankin bound test point selection

The BB is valid for any choice of test points $\boldsymbol{\eta}_i$ ($i = 1, 2, \ldots, L$) inside the parameter space. However, it is better to obtain the BB as tight as possible. In our problem, the parameter space is $[l, m, \sigma_s^2, \sigma_n^2] \in (-1, 1) \times (-1, 1) \times (0, +\infty) \times (0, +\infty)$. We choose the test points to be the sidelobes of each unknown parameter. This is because the level of sidelobe reflects the probability of estimation ambiguity. In consideration of the existence of coupling effects between the source positions l and m, the test points of l and m are chosen as the sidelobes of the plan (l, m). For the source intensity σ_s^2 and the noise intensity σ_n^2, since there exists no sidelobe, we will just choose several test points in the vicinity of the true values. More specifically, the test points for σ_s^2 and σ_n^2 are $(0.9, 0.99, 1.1)\sigma_s^2$ and $(0.9, 0.99, 1.1)\sigma_n^2$. In the following numerical experiments, the numbers of test points for (l, m), σ_s^2, and σ_n^2 are 20, 3, and 3, respectively.

V. SIMULATION RESULTS

The whole simulation consists of two parts: the antenna selection stage and the array performance evaluation stage.

A. Antenna selection

A four-branch cross array is considered in our simulation, in which each branch is a ten-element half-wavelength spaced uniform linear array (ULA), i.e., $p = 40$. The budget for antenna selection is set to K = 3 for each branch, resulting in a total of 12 antennas being selected from the candidate array. The source position is set at (0,0), allowing for the search of a symmetric array. To simplify the selection process, we only conduct the antenna selection scheme on one branch and replicate the results on the other three branches.

It is worth mentioning that at high SNR, the BB coincides with the CRB and is equivalent as a design criterion. However, at lower SNR, the BB is a more relevant criterion than the CRB because of the consideration of the threshold effect. For the antenna selection stage, we set the SNR to -10dB, where SNR is defined as $10\log_{10}(\sigma_s^2/\sigma_n^2)$ and σ_n^2 is fixed as 1.
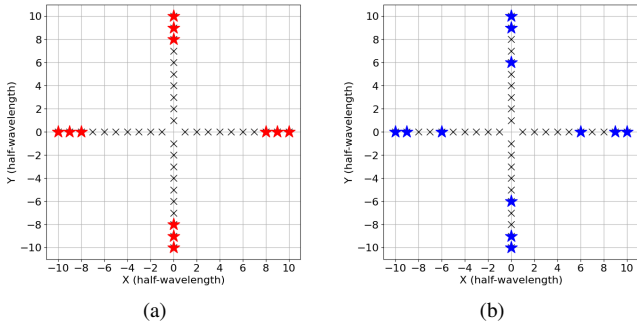
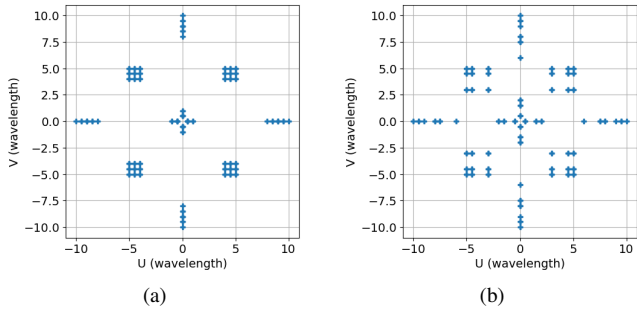Fig. 1: The antenna array given by (a) CRB-based criterion, (b) BB-based criterion.

Fig. 2: The UV plane coverage of the array given by (a) CRB-based criterion, (b) BB-based criterion.
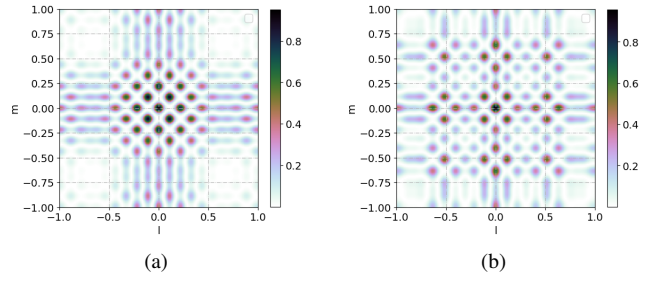

Fig. 3: (a) The 2D beampattern of the array given by CRB-based criterion. (b) The 2D beampattern of the array given by BB-based criterion.
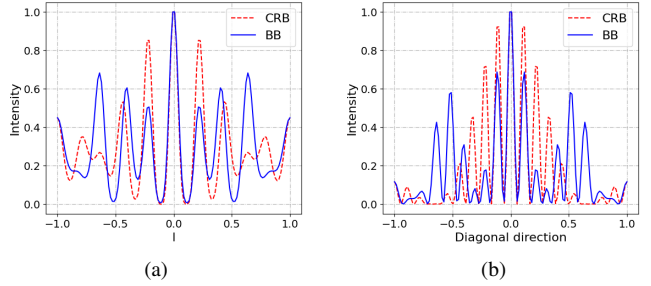

Fig. 4: (a) The 1D beampattern of the l-direction. (b) The 1D beampattern of the diagonal direction. Red dashed (blue solid) lines represent the result of the array geometries given by CRB (BB)-based optimization criteria.

B. Array performance evaluation

Fig. 1 presents the antenna array selection results of CRB- and BB-based criteria. Notably, all the antennas of the CRB-optimal array geometry are located at the border of the possible positions. This result coincides well with the known property that the CRB is a local bound, focusing on the array's resolution (leading to a thinner mainlobe). However, this type of array typically results in higher sidelobe levels. In contrast, the BB criterion leads to only two antennas placed at the border of the cross branch, ensuring the maximum aperture, with others located elsewhere to control sidelobe levels. This can be explained by the use of several test points over the entire parameter space, which takes into account the ambiguity effect of the array.

The UV plane coverage of the two geometries is illustrated in Fig. 2. The UV plane coverage represents the collection of all baselines, i.e., the distance vector between two antennas, and is crucial in radio interferometry as it determines the interferometer's ability to capture different angular scales on the sky. It can be observed that the coverage of the BB-optimal array spreads out more and is more concentric than that of the CRB-optimal array. Thus, the BB-optimal array provides better UV plane coverage.

Fig. 3 gives the beampatterns of the two array geometries. Since it is quite difficult to compare directly the 2D beampatterns, two special axes are selected to better illustrate the beampattern in 1D: the l-direction and the diagonal direction

($l = m$), which are shown in Fig. 4. It is worth noting that for the beampattern of CRB-optimal geometry, the mainlobe is very thin, but at the same time the sidelobe level is also very high. In contrast, the mainlobe of the BB-optimal array is little wider, whereas the management of the sidelobe is considerably improved, especially in the diagonal direction.

With the purpose of assessing the performance of the two array geometries, those CRB and BB are calculated and shown in Fig. 5 as a function of the SNR. For comparison, the performance of the maximum likelihood (ML) estimator is evaluated by performing 15000 Monte Carlo simulations. For the reason that the corresponding bounds and MSEs on m estimation are the same as those on l estimation, only the results on l estimation are shown in Fig. 5. For both arrays, the behavior of the BB well reflects that of the MSE, where the difference in the predicted SNR threshold given by BB is around 10dB below that of the ML. Notably, the threshold SNR of the array given by the BB-based criterion is almost 5dB smaller than that of the CRB-based criterion, indicating that the BB-based criterion yields better performance in the SNR transition region. As a result, using the BB-based criterion can increase the asymptotical region of the array by 5dB, from 3dB to -2dB.

The CRB, BB and MSEs on σ_s^2 estimation of the two arrays obtained by CRB- and BB-based design criteria are revealed in Fig. 6. It is worth noting that there is no difference between the two arrays' estimation performances in terms of CRB, BB or MSE. It means that the objective of optimizing simultaneously
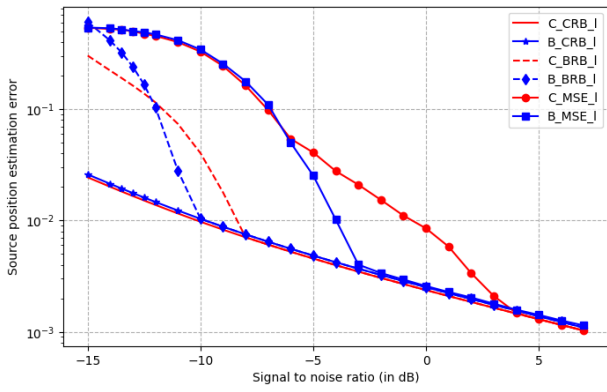
Fig. 5: Bounds and MSEs on l estimation. Solid lines, dashed lines, and solid lines with points markers in red (blue) represent the CRB, BB, and MSEs of the array geometries given by CRB (BB)-based optimization criteria.

Fig. 6: Bounds and MSE on σ_s^2 estimation. Solid lines, dashed lines, and solid lines with points markers in red (blue) represent the CRB, BB, and MSEs of the array geometries given by CRB (BB)-based optimization criteria.
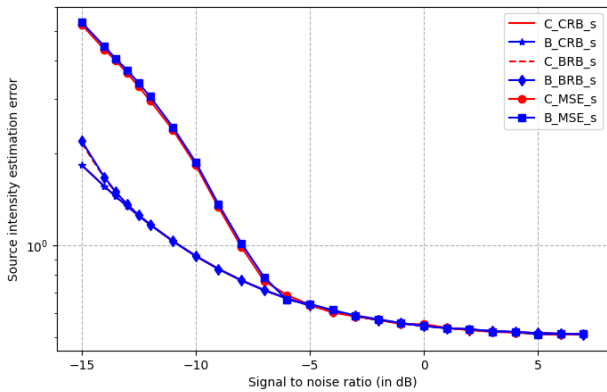
the estimation on source location (l, m) and intensity σ_s^2 is achieved. In essence, compared with the CRB-based criterion, the BB-based criterion can significantly improve the source position estimation performance in the SNR transition area while ensuring the estimation performance on the intensity.

Remark: Given that the threshold SNR predicted by BB is always lower than that of the MSE, we opted to conduct the antenna array selection at an SNR of -10dB (threshold given by BB). As expected, this led to an improvement in the performance of the resulting array at the SNR transition area, from -5dB to 3dB, which is the range where the array is expected to be used.

VI. CONCLUSIONS

In this paper, the antenna array selection problem is investigated. The CRB- and BB-based optimization criteria are compared. The CRB, BB and MSE are calculated to evaluate the performance of the two optimized array geometries. The simulation results have shown that the BB is a more

appropriate criterion than the CRB at low SNR by improving the estimation performance in the SNR transition region. The BB allows for obtaining a trade-off between the mainlobe width and sidelobe levels, achieving a good precision of estimation while reducing ambiguity. Ongoing work consists of developing efficient and low computational cost optimization strategies for more general arrays.

REFERENCES

[1] "NenUFAR," https://nenufar.obs-nancay.fr/, [Online].
[2] "Square kilometre array." https://www.skatelescope.org/, [Online].
[3] S. Liu, S. P. Chepuri, M. Fardad, E. Maşazade, G. Leus, and P. K. Varshney, "Sensor selection for estimation with correlated measurement noise," *IEEE Transactions on Signal Processing*, vol. 64, no. 13, pp. 3509–3522, 2016.
[4] S. Joshi and S. Boyd, "Sensor selection via convex optimization," *IEEE Transactions on Signal Processing*, vol. 57, no. 2, pp. 451–462, 2008.
[5] M. Juhlin and A. Jakobsson, "Optimal sensor placement for localizing structured signal sources," *Signal Processing*, p. 108679, 2022.
[6] J. P. Delmas, M. N. El Korso, H. Gazzah, and M. Castella, "CRB analysis of planar antenna arrays for optimizing near-field source localization," *Signal Processing*, vol. 127, pp. 117–134, 2016.
[7] M. Juhlin and A. Jakobsson, "Optimal microphone placement for localizing tonal sound sources," in *2020 28th European Signal Processing Conference (EUSIPCO)*. IEEE, 2021, pp. 236–240.
[8] M. N. El Korso, A. Renaux, R. Boyer, and S. Marcos, "Deterministic performance bounds on the mean square error for near field source localization," *IEEE transactions on signal processing*, vol. 61, no. 4, pp. 871–877, 2012.
[9] P. Zarka, M. Tagger, L. Denis, J. Girard, A. Konovalenko, M. Atemkeng, M. Arnaud, S. Azarian, M. Barsuglia, A. Bonafede *et al.*, "NenUFAR: Instrument description and science case," in *2015 International Conference on Antenna Theory and Techniques (ICATT)*. IEEE, 2015, pp. 1–6.
[10] V. Ollier, M. N. El Korso, R. Boyer, P. Larzabal, and M. Pesavento, "Robust calibration of radio interferometers in non-gaussian environment," *IEEE Transactions on Signal Processing*, vol. 65, no. 21, pp. 5649–5660, 2017.
[11] V. Ollier, M. N. El Korso, A. Ferrari, R. Boyer, and P. Larzabal, "Robust distributed calibration of radio interferometers with direction dependent distortions," *Signal Processing*, vol. 153, pp. 348–354, 2018.
[12] M. Morelande and B. Ristic, "Signal-to-noise ratio threshold effect in track before detect," *IET radar, sonar & navigation*, vol. 3, no. 6, pp. 601–608, 2009.
[13] R. McAulay and L. Seidman, "A useful form of the Barankin lower bound and its application to PPM threshold analysis," *IEEE Transactions on Information Theory*, vol. 15, no. 2, pp. 273–279, 1969.
[14] J. M. Hammersley, "On estimating restricted parameters," *Journal of the Royal Statistical Society. Series B (Methodological)*, vol. 12, no. 2, pp. 192–240, 1950.
[15] R. McAulay and E. Hofstetter, "Barankin bounds on parameter estimation," *IEEE Transactions on Information Theory*, vol. 17, no. 6, pp. 669–676, 1971.
[16] J. Tabrikian, O. Isaacs, and I. Bilik, "Cognitive antenna selection for automotive radar using bobrovsky-zakai bound," *IEEE Journal of Selected Topics in Signal Processing*, vol. 15, no. 4, pp. 892–903, 2021.
[17] A. R. Thompson, J. M. Moran, and G. W. Swenson, *Interferometry and synthesis in radio astronomy*. Springer Nature, 2017.
[18] K. Todros and J. Tabrikian, "General classes of performance lower bounds for parameter estimation—Part I: Non-Bayesian bounds for unbiased estimators," *IEEE Transactions on Information Theory*, vol. 56, no. 10, pp. 5045–5063, 2010.
[19] S. J. Wijnholds and A.-J. van der Veen, "Fundamental imaging limits of radio telescope arrays," *IEEE Journal of Selected Topics in Signal Processing*, vol. 2, no. 5, pp. 613–623, 2008.
[20] A. Quinlan, E. Chaumette, and P. Larzabal, "A direct method to generate approximations of the Barankin bound," in *2006 IEEE International Conference on Acoustics Speech and Signal Processing Proceedings*, vol. 3. IEEE, 2006, pp. 3259–3262.
[21] S. P. Chepuri and G. Leus, "Sparsity-promoting sensor selection for non-linear measurement models," *IEEE Transactions on Signal Processing*, vol. 63, no. 3, pp. 684–698, 2014.